

Non-Intersecting Leaf Insertion Algorithm for Tree Structure Models

Journal:	<i>Interface Focus</i>
Manuscript ID	RSFS-2017-0045.R1
Article Type:	Research
Date Submitted by the Author:	07-Dec-2017
Complete List of Authors:	Åkerblom, Markku; Tampere University of Technology, Laboratory of Mathematics Raumonon, Pasi; Tampere University of Technology, Laboratory of Mathematics Casella, Eric; Forest Research, Centre for Sustainable Forestry and Climate Change Disney, Mat; University College London, Geography; Danson, Francis; University of Salford, School of Environmenta and Life Sciences Gaulton, Rachel; Newcastle University, School of Civil Engineering and Geosciences Schofield, Lucy; York St John University, School of Humanities, Religion and Philosophy Kaasalainen, Mikko; Tampere University of Technology, Laboratory of Mathematics
Subject:	Biomathematics < CROSS-DISCIPLINARY SCIENCES, Computational biology < CROSS-DISCIPLINARY SCIENCES, Mathematical physics < CROSS-DISCIPLINARY SCIENCES
Keywords:	leaf insertion, leaf distribution, quantitative structure model, laser scanning, tree reconstruction

Non-Intersecting Leaf Insertion Algorithm for Tree Structure Models

December 7, 2017

Markku Åkerblom*¹, Pasi Raunonen¹, Eric Casella², Mathias Disney³, F. Mark Danson⁴,
Rachel Gaulton⁵, Lucy A. Schofield⁶, and Mikko Kaasalainen¹

¹ Laboratory of Mathematics, Tampere University of Technology, P.O. Box 553, 33101, Tampere, Finland

² Centre for Sustainable Forestry and Climate Change, Forest Research, Farnham, GU10 4LH, UK

³ UCL Department of Geography, Gower Street, London WC1E 6BT, UK; and NERC National Centre for Earth Observation (NCEO), UK.

⁴ School of Environment and Life Sciences, University of Salford, Salford M5 4WT, UK

⁵ School of Civil Engineering and Geosciences, Newcastle University, Newcastle upon Tyne, NE1 7RU, UK

⁶ School of Humanities, Religion & Philosophy, York St John University, YO31 7EX, UK

* Corresponding author markku.akerblom@tut.fi

Abstract

We present an algorithm and an implementation to insert broadleaves or needleleaves to a quantitative structure model according to an arbitrary distribution, and a data structure to store the required information efficiently. A structure model contains the geometry and branching structure of a tree. The purpose of the work is to offer a tool for making more realistic simulations with tree models with leaves, particularly for tree models developed from terrestrial laser scan (TLS) measurements. We demonstrate leaf insertion using cylinder-based structure models, but the associated software implementation is written in a way that enables the easy use of other types of structure models. Distributions controlling leaf location, size and angles as well as the shape of individual leaves are user-definable, allowing any type of distribution. The leaf generation process consist of two stages, the first of which generates individual leaf geometry following the input distributions, while in the other stage intersections are prevented by doing transformations when

1
2 28 required. Initial testing was carried out on English oak trees to demonstrate the approach and
3
4 29 to assess the required computational resources. Depending on the size and complexity of the
5
6 30 tree, leaf generation takes between 6 and 18 minutes. Various leaf area density distributions were
7
8 31 defined, and the resulting leaf covers were compared to manual leaf harvesting measurements.
9
10 32 The results are not conclusive, but they show great potential for the method. In the future, if our
11
12 33 method is demonstrated to work well for TLS data from multiple tree types, the approach is likely
13
14 34 to be very useful for 3D structure and radiative transfer simulation applications, including remote
15
16 35 sensing, ecology and forestry, among others.

17 36 **Keywords:** leaf insertion, leaf distribution, quantitative structure model, laser scanning, tree re-
18
19 37 construction

20 21 38 **1 Introduction**

22
23
24 39 Leaves and needles are essential for the functioning of plants and their interaction with the envi-
25
26 40 ronment. They are also the main part of the vegetation interacting with remote sensing measure-
27
28 41 ments. Thus, the ability to measure and model leaf distributions of plants has great importance
29
30 42 and many applications in ecology, forest research and remote sensing [1, 2, 3].

31 43 We will present an algorithm to generate a leaf cover on any plant structure model with any un-
32
33 44 derlying distribution for the leaf parameters. Although, the process could be utilized with any types
34
35 45 of plants, this publication focuses only of trees. The leaf parameter distributions are supported by
36
37 46 quantitative structure models (QSM) of trees, and the generated leaves are non-intersecting. This
38
39 47 allows, among other things, the use of more realistic leaf distributions in gap fraction and radiative
40
41 48 transfer based simulations, in comparison to the previously suggested uniform layers of possibly
42
43 49 intersecting leaves [4].

44 50 The above-ground biomass of a tree consists mainly of leaves, and woody material in the trunk
45
46 51 and branches. In recent years various methods have been presented to reconstruct the woody
47
48 52 parts of a tree in a quantitative manner from terrestrial laser scanning (TLS) data [5, 6]. Further-
49
50 53 more, it is possible to estimate foliage distribution from similar data [7] (for further information, see
51
52 54 [8]). However, reconstructing both the woody and leaf parts at the same time is more challeng-
53
54 55 ing due to self-occlusion effects, and the complex nature of leaf-wood separation from TLS data,
55
56 56 which has been studied extensively [9, 10].

57 57 An alternative to *extracting* the leaves from TLS data is scanning the tree during leaf-off sea-
58
59 58 son, and then trying to *insert* leaves after reconstructing the woody structure. To generate a leaf
60
61 59 cover statistically similar to the original, certain leaf property distributions have to be estimated
60
61 60 [11]. Such approaches do not aim to reconstruct real leaves but rather the underlying leaf distri-
61
62 60 bution, which can be sampled to produce leaf covers that are statistically similar to the real one.

1
2 62 The approach is limited to deciduous, broadleaf canopies. However, from this we may learn how
3
4 63 to improve and develop methods for separation and re-insertion of green material in evergreen
5
6 64 broadleaf and needleleaf trees.

7 65 Measuring leaf position, size and orientation by hand is extremely laborious [11] as one can
8
9 66 have millions of leaves per tree. Great progress has achieved remote sensing to detect leaf prop-
10
11 67 erties. Methods have been presented to estimate the 3D distribution of leaf material from TLS data
12
13 68 [7, 12]. Furthermore, methods for measuring leaf orientation distribution from similar data have
14
15 69 been presented by [13] and more recently by [14]. Determining leaf size distribution remotely is
16
17 70 more challenging as it requires the detection of leaf edges [15], which is also challenging due to
18
19 71 the decrease in data point density higher in the canopies, when scanning from the ground. How-
20
21 72 ever, sampling leaf size by hand is faster and less error-prone than leaf angle, especially when
22
23 73 carried out in a destructive manner.

24 74 The algorithm we present in this paper populates a QSM of the woody parts of a tree with
25
26 75 leaves, resulting in a model with inserted leaves (L-QSM). The algorithm generates leaves based
27
28 76 on user-defined leaf property distributions that may be estimated with the methods presented
29
30 77 above, or alternatively by using distributions parametrized by branch properties such as branch
31
32 78 order. Basic steps of the procedure are illustrated in Fig. 1, which shows an example leaf area
33
34 79 distribution supported by a QSM, leaves generated by sampling the distribution, and the final
35
36 80 product which is a L-QSM.

37 81 The algorithm is designed to work with models consisting of any type of geometry, but we use
38
39 82 models that are a collection of cylinders, *i.e.*, cylindrical QSMs [5]. The leaf insertion procedure
40
41 83 works on *blocks*, which is essentially the largest unit of the structure model that can be assumed
42
43 84 to have uniform leaf distribution parameters that can define, *e.g.*, limits for the number of leaves,
44
45 85 leaf size and orientation. Because certain tree species can have a different leaf density along
46
47 86 branches, the blocks can be smaller than the branch. Thus, the cylinders forming the QSM geom-
48
49 87 etry, and other similar small geometric primitives [16], can be used directly as blocks. However, it
50
51 88 would also be possible to divide the cylinders and form even smaller blocks. In the case of voxel-
52
53 89 based structure models a pre-processing step is required to form blocks that are a collection of
54
55 90 voxels. Similarly, in continuous surface models the branch surfaces should be divided into smaller
56
57 91 sections that can be used as blocks.

58 92 As the leaf insertion algorithm is designed to be as general as possible, *i.e.*, any user-defined
59
60 93 distribution can be used, validation can take various forms. We carry out initial validation using leaf
61
62 94 area and count measurements from three English Oaks together with their QSMs reconstructed
63
64 95 from TLS data. Both the TLS and leaf measurements are presented in Sect. 2.1. The structure
65
66 96 reconstruction process to create the required cylindrical QSMs is briefly described in Sect. 2.2.

67 97 The leaf insertion algorithm is presented in Sect. 2.3 together with the related distributions that

control leaf position, size and orientation. Although this paper focuses on sampling the described distributions to produce individual leaves with a known geometry, it is not always necessary as discussed in Sect. 2.4. The section shows how the distributions define a leaf density distribution around the structure model blocks, and how that overall distribution can be used for computations without generating the geometry of individual leaves. Although we focus on broadleaves, the procedure can be used also for generating needles. Approaches for working with needles are presented in Sect. 2.5.

A MATLAB implementation of the algorithm, including descriptions of the related classes and the main function, is introduced in Sect. 2.6. The MATLAB implementation was used to compute several leaf distributions for the oak trees. The results are presented in Sect. 3. Discussion is included in Sect. 4 and conclusions are made in Sect. 5.

2 Materials and methods

2.1 Laser scanning and leaf measurements

Our analysis was based on raw point-clouds recorded at Alice Holt Forest, UK (51.1533 N, 0.8512 W) by a single-return phase-shift Leica HDS-6100 TLS (Leica Geosystems Ltd., Heerbrugg) on three 80-year-old oak trees (*Quercus robur* L.). Scans were performed in March 2014, during winter-time, in dry and low wind speed (less than 1 ms^{-1}) conditions. Trees were recorded from six scan positions around each tree (azimuth angle of 0-South, 60, 120, 180, 240 and 300°) at a distance of 5 m from the base of the tree and with a TLS sampling resolution level of 0.018° at each scan position. Six reflective targets were set out around each tree to merge the multiple scans. 3D reconstructions of the trees were then computer-generated using the method described in [5].

The trees were harvested in June 2014. The foliage sampling method consisted of a manually stripping off each leaf from the branches and storage in bags giving the height stratum to which they belonged (see Table 1). A second component of the method involved the collection of a set of 100 leaves at random from each stratum on each tree. Each stratum-bag was then fresh-weighed (Avery Berkel HL206, UK) and oven dried at 75°C to obtain their dry masses. From the sub-sets, individual leaf area was measured in the laboratory with a laser area meter (CID-203, Camas, WA) and weighed (Mettler Toledo AG204, Switzerland) before and after oven drying at 75°C . Specific Leaf Area (SLA) was derived for each of the sub-sets and used to estimate the total leaf area and the number of leaves for each stratum after e.g., [17, 12]. Additionally, the average area of the leaves was recorded from the smallest to the largest tree as 33.71, 40.33 and 29.66 cm^2 , respectively.

2.2 Quantitative structure models

The three oak trees were reconstructed as cylindrical QSMs in MATLAB with the procedure detailed in [18]. The properties of the resulting models are listed in Table 2. Furthermore, the branch count distribution per branch order is visualized in Fig. 2. The count of the branches is important as leaves are placed near the tips of the branches.

The small and medium oaks were similar in height, but the latter had about 2.6 times more branches when measured in total count and in length. The large oak had the most branches for all branch orders, and almost twice the volume of the medium oak.

2.3 Leaf generation algorithm

This section describes an algorithm to populate QSMs with leaves. The main inputs of the algorithm are distributions that control the position, orientation, and size of the leaves. These distributions are sampled to retrieve the parameters of individual leaves. The approach can be described as simplified, or naïve, for three reasons: 1) position, orientation and size are sampled independently, which is to say that, *e.g.*, the size of a leaf may not affect its orientation; 2) simple controls for phyllotaxy and clumping effects are yet to be implemented (although there is some control when generating the petioles); and 3) the only effect leaves have on one another is that they are prevented from intersecting. We call this procedure the *Foliage and Needles Naïve Insertion* algorithm, or the FaNNI-algorithm in short.

2.3.1 Overview of the procedure

The inputs of the algorithm are a collection of QSM blocks, leaf basis geometry, target leaf area to be distributed, and petiole and leaf parameter distributions. Details of the roles of the leaf basis geometry and the distributions are presented in Sects. 2.3.2 and 2.3.3, respectively. The process can be viewed as two separate stages: I) generating candidate leaves, II) accepting candidates while preventing intersections. An overview of the process is provided in Fig. 3.

The first stage begins by distributing the available leaf area onto the blocks. The leaf area density distribution (LADD) determines the relative probability for a block with given parameters to have leaf area. After sampling the distribution with the block properties, each block has a target leaf area, or a leaf area budget, that will be divided into individual leaves by sampling the leaf size distribution (LSD).

For the leaf size determination the blocks are processed in random order. To match the target leaf area as closely as possible the cumulative area difference with respect to the target is updated after each leaf. While there is room in the current block, or the cumulative area budget, a new leaf is added to that block. The algorithm assumes that all the generated leaves have the same

1
2 163 geometry, and thus we can sample a leaf length value which can be converted to area. After this
3
4 164 step, the number of generated leaves and the block parent of each leaf are known.

5 165 Next, the locations of the leaves are determined by physically attaching them to their branches
6
7 166 by the petioles. Because TLS measurements usually cannot capture petioles as they are too small
8
9 167 to be detected reliably, all the petioles are generated: The petiole's starting point, orientation and
10 168 length are determined by sampling appropriate parameter distributions given by the user. The
11
12 169 end point of a petiole also determines the origin of the respective leaf. Although the exact petiole
13
14 170 geometry is computed, they are considered insignificant compared to the blocks and the leaves,
15 171 and thus they are excluded later from the intersection detection process.

16 172 The final property to sample is the leaf orientation. The leaf orientation distribution (LOD) is
17
18 173 used to determine the direction and the surface normal of each leaf. Once this is done, all leaves
19
20 174 have a fixed position, orientation and scale, and their geometry can be computed by transforming
21
22 175 the leaf basis geometry accordingly.

23 176 At this point it is possible, and even likely with a high leaf count, that some of the leaf candidates
24
25 177 intersect one another, or with the blocks, as they were generated independently. However, the
26
27 178 goal is to produce a model without leaf intersections, and thus in the second stage the leaves are
28 179 checked one-by-one for intersections before adding them to the list of accepted leaves.

29 180 If a leaf candidate intersects a block or an accepted leaf, it is possible to try to change the
30
31 181 position, orientation and scale of the leaf and check whether the intersection was avoided. If it
32
33 182 was, the leaf candidate is accepted, if not, the process can be repeated any number of times with
34
35 183 a different transformation applied to the parameters. If despite all the transformations, intersections
36 184 cannot be avoided the candidate is discarded. An example of how intersection prevention can be
37
38 185 implemented is described in Sect. 2.3.4. The leaf generation process stops when all the leaves
39 186 have been processed, unless some other stopping condition has been given, such as a target leaf
40
41 187 area of accepted leaves.

42 43 44 188 **2.3.2 Leaf model**

45
46 189 The leaf model defines the basis geometry of an individual leaf. This geometry is the same for
47
48 190 all the sampled leaves, but it is scaled, rotated and translated to receive the final leaf geome-
49
50 191 try, during the generation process. Thus all the generated leaves have the same shape but the
51
52 192 size and orientation can vary. In the simplest case, the basis geometry can be a single triangle,
53
54 193 allowing fast leaf cover generation due to simple intersection detections. For examples of basis
55
56 194 geometries consisting of triangles, see Sect. 2.6. On the other hand, there is no upper limit for
57
58 195 the complexity of the basis geometry, other than computational time requirements to ensure non-
59
60 196 intersecting leaves. Thus, it is possible to represent more complicated shapes, *e.g.*, a leaf with
197 three-dimensional curvature, or a compound-leaf with several leaflets, that do not have to lie on

1
2 198 the same plane. However, to simplify the generation process, it is possible to use a simplified basis
3
4 199 geometry while generating the leaves, which is then replaced with something more complex, as
5
6 200 long as the change does not introduce additional intersections.

7 201 The origin of the leaf basis coordinate system is assumed to be the point where the petiole
8
9 202 connects to the leaf. Leaf *direction* is the direction from the origin towards the tip of the leaf, and
10
11 203 perpendicular to this lies the leaf *normal* that defines the direction to which (most of) the leaf area
12
13 204 is facing. The length of the basis geometry, *i.e.* leaf length, is fixed at unity. Other dimensions
14
15 205 are given in respect to that. During leaf parameter sampling only the leaf length is sampled as it
16
17 206 determines the leaf area when the basis geometry is fixed. Note that it is not required to compute
18
19 207 the exact geometry of the leaf candidates before intersection prevention stage.

20 208 **2.3.3 Leaf and petiole parameter distributions**

21
22 209 Leaf and petiole properties are controlled by multiple user-definable distributions which are sam-
23
24 210 pled when leaves are generated. The properties fix the number of leaves, their position, size and
25
26 211 orientation. In theory, these distributions are multidimensional as they may depend on any number
27
28 212 of block properties, such as height from ground, radius and orientation. They can also be formed
29
30 213 as a weighted product or sum of one-dimensional marginal distributions. The purpose of each
31
32 214 distribution is described below in the order they are sampled in the implementation.

33 215 **Leaf area density distribution (LADD)** Total leaf area is one of the inputs of the algorithm,
34
35 216 and leaf area density distribution defines how that area should be distributed to the blocks. Thus,
36
37 217 the leaf area density distribution can allocate more leaf area towards the top of the tree and towards
38
39 218 the tips of the branches. One could also prevent leaf area being attached directly to stem blocks
40
41 219 by using branch order information. Furthermore, the distribution produces a relative mapping of
42
43 220 area on the blocks, allowing the distribution to assign any given total area of leaves to the structure
44
45 221 model.

46 222 **Leaf size distribution (LSD)** After a leaf area target has been assigned to each block, the
47
48 223 leaf size distribution is used to sample leaf count and size, so that the target area is matched
49
50 224 as closely as possible. This distribution determines the number of leaves to be generated N_{init} .
51
52 225 However, as no intersections between leaves or between blocks and leaves are tolerated, the final
53
54 226 number of leaves may be smaller than initially generated if intersection can not be avoided with
55
56 227 transformations, *i.e.* $N_{final} \leq N_{init}$ holds.

57 228 **Petiole generation** After size distribution sampling, the number of leaves is known and it be-
58
59 229 comes possible to sample the petioles that connect the leaves to their block parents. Similarly to
60

leaves, petiole parameters include the starting point, orientation and length of the petiole, which effectively also determine the starting points, or origins, of the leaves. It would be possible to model the petioles as 3D objects, like small cylinders, but the implementation considers them only as line segments, and they are excluded from the intersection prevention step.

Leaf orientation distribution (LOD) The final distribution controls the orientation of the leaves. This distribution controls the directions and normals of the leaves, and can be used to describe, *e.g.*, which parts of the tree are *erectophile* and which are *planophile*.

2.3.4 Intersection prevention

Sampling the presented leaf and petiole parameter distributions results in a list of N_{init} candidate leaves. But because each sample is independent of the rest, the leaves may intersect with other leaves in the list, or blocks of the QSM. To avoid intersections, leaves are only accepted to the final collection of leaves if they do not intersect with other geometry.

The accepted leaves list is initialized as empty. One-by-one, the initial leaves are checked, so that they do not intersect with any of the blocks or the accepted leaves. To avoid a low acceptance rate, an intersecting leaf is not discarded instantly. Instead a number of preselected user-defined transformations are applied to the leaf candidate, and intersection checking is repeated. A transformation may consist of any combination of scaling, rotation and translation, but they are applied in that order. Only if none of the preselected transformations prevent all the intersections, the candidate is discarded.

2.4 Leaf density model

Sect. 2.3 described an algorithm to generate exact leaf geometry by sampling certain distributions that depended on individual block parameters. However, in some cases it is not necessary to compute the exact geometry, but rather to view the leaves as an abstract density around the branches [19]. Such an approach saves computational resources as there is no need to compute and store a lot of geometry. This is especially relevant for computations with needles as their number often far exceeds the number of broadleaves for similar sized trees. This abstract approach without exact leaf realizations can be suitable for many applications, *e.g.*, ray tracing operations in radiative transfer and gap fraction computations. However, exact geometry may be better suited for some applications, *e.g.*, requiring realistic visualization, and it is also a more straight-forward way to study effects on a single broadleaf of needle scale.

The distributions defined earlier depended on block properties which essentially means, that each block defines a density, size and angle distribution around itself. In the case of a cylindrical QSM, this can be viewed as a *leaf density cylinder* around the block (See Fig. 4). The radius

(and length) of the leaf cylinder is defined by petiole length and leaf size distributions. Let us next briefly justify the leaf cylinders as potentially useful and consider ray tracing with leaf cylinders as an example. One possible approach for ray tracing applications would be to determine an absorption rate for the leaf cylinder, which can depend on distance from the cylinder axis, and where the rate can be stochastic (*cf.* the turbid medium analogy [4]). Branch cylinders can be viewed as infinitely dense, and thus hits occur at their surface. When enough of the energy of a simulated beam is absorbed, a hit occurs inside a leaf cylinder. If the application requires it, an incidence angle can be sampled from the orientation distribution stored in the respective block.

2.5 Inserting needles

Although this paper focuses on demonstrating broadleaf insertion, it is possible to use the algorithm with needles in different ways. The most obvious method is to use a tiny cylinder to represent a single needle and use that as a basis geometry. However, the computational requirements of the insertion would be enormous (but not impossible [20]), as they would be for any further application using the resulting model.

A less resource-consuming approach would be a modification of the leaf density cylinder approach described in Sect. 2.4. Rather than inserting needles at all, they could be viewed as a density distribution around the blocks (*cf.* [19]). Note that the distribution does not have to be uniform, and thus it can be used to account for needle phyllotaxy. Additional buds could also be introduced as density cylinders if the QSM does not contain the level of details in terms of branching structure required by the user. Even though exact needle geometry is not generated, it is important to incorporate the needle phyllotaxy in any ray tracing operations inside needle density cylinders, as it is key in simulations including needles [21].

A third option would be to use a needle bud as the basis geometry. An example needle bud suitable for visualization applications can be seen in Fig. 5. Even though the model is complex, it can be simplified to a cylinder during the intersection checking stage. The complex model can still be used for visualizations, or in further computations when required.

2.6 A MATLAB implementation

The leaf insertion algorithm was implemented in MATLAB [22]. The supporting classes and the main function of the implementation are presented below. Currently the implementation works with leaves, where the basis geometry is a collection of triangles, and cylindrical QSMs, but the structure of the implementation is modular, so that it is easy to extend to other types of leaves and blocks as necessary.

2.6.1 Classes

The following classes were written to make the implementation as modular as possible. Especially, the `LeafModel` and `QSMB` abstract classes were designed to define interfaces for easy extendibility when using other structures than cylindrical QSMs, or triangle-based leaf models.

LeafModel The objects of this class have two main purposes in terms of the data they hold. First they contain the leaf basis geometry, that is transformed to determine the geometry of generated leaves. Secondly, they hold the parameters of the accepted leaves, *i.e.*, leaf origin, scale, direction and normal. In terms of functionality the class is responsible for defining an intersection detection method for two leaves. There is also a method for converting the geometry of a leaf into a collection of triangles. The `triangles` method is required mainly when detecting intersections between a leaf and a block.¹ There is also a method for adding a new, accepted leaf to the model.

`LeafModel` is an abstract class, used only for defining the required interface for subclasses rather than actually creating instances. This allows the class to be extended by creating subclasses, such as, the implemented `LeafModelTriangle` class for leaf models, where the leaf basis geometry consists of vertices and triangular faces. This class already allows numerous leaf shapes, as seen in Fig. 6, but the user can extend the possibilities by implementing a subclass of `LeafModel`, *e.g.*, for leaf geometry defined with Bézier curves, or other vertex–face based geometries but with more optimized intersection detection than checking each triangle separately.

QSMB The class name is an acronym for Quantitative Structure Model Blocks, and it essentially acts as a container for QSM block information. The class is abstract and used to define an interface for its subclasses. The interface includes a method for reading block properties, such as position, orientation and branch order, and to detect intersection between blocks and triangles. Furthermore, a `QSMB` object is responsible for generating the petioles of the leaves using the block geometry. Finally, there is a method for converting the blocks of a QSM into a `CubeVoxelization` object, which is used to optimize intersection detection.

As an example subclass, the `QSMBCylindrical` was created to contain cylindrical QSM data. In this class the block data consist of cylinder parameters for the geometry, and branching topology, such as, branch order information. The user can extend the implementation to work on other types of structure models, by providing the appropriate subclass definition.

The `QSMBCylindrical` class also defines default uniform distributions for the petiole parameters. In this initial implementation the petiole parameters are the following, with the lower and upper limits in parenthesis: relative position along cylinder axis (0, 1); relative position in radial direction when connected to the end circle of the last cylinder in a branch (0, 1); rotation around

¹Otherwise you would have to write a separate intersection detection function for each leaf and block type pair.

1
2 328 cylinder axis $(-\pi, \pi)$; petiole elevation $(-\frac{\pi}{2}, \frac{\pi}{2})$; petiole azimuth $(-\frac{\pi}{2}, \frac{\pi}{2})$; and petiole length (2 cm,
3
4 329 5 cm).

5
6
7 330 **CubeVoxelization** An object of this class is a voxelization of a fixed 3D space into cubical
8 331 voxels with a fixed edge length. A `CubeVoxelization` object has a minimum and a maximum point
9
10 332 and the space between them is divided into a finite number of cells. Object references can be
11 333 stored into the cells to indicate that the objects occupy at least a part of that voxel. In the main
12
13 334 function of the leaf insertion implementation, voxelizations are used to store and find candidate
14
15 335 leaves and blocks, to perform more accurate intersection detection. Furthermore, the edge length
16 336 of the voxelizations is set as the maximum leaf size produced by sampling the leaf size distribution
17
18 337 function.

21 338 2.6.2 Main function

22
23 339 `qsm_fanni` is the main function that receives the QSM as a `QSM` object, an initialized `LeafModel`
24 340 object that contains the leaf basis geometry, and total leaf area to be distributed. The leaf area
25 341 parameter can have two components; one for the initial leaf area A_{init} to be generated, and one for
26
27 342 the target leaf area $A_{target} \leq A_{init}$. This can be used to increase the probability that the target area
28
29 343 is reached, even if some of the generated leaves are discarded due to unavoidable intersections.

30
31 344 There are also numerous optional inputs for the user to customize, such as the distribution
32
33 345 functions and transformations during the intersection prevention step. However, default options
34
35 346 are available for all the remaining parameters.

36 347 The main output of the function is a `LeafModel` object derived from the corresponding input,
37
38 348 but it now contains the accepted leaves, petiole start points, and a vector of parent block indices
39
40 349 of each accepted leaf.

41 42 43 350 2.6.3 Default leaf parameter distributions

44
45 351 The implementation contains default distribution functions for leaf parameter properties, and they
46
47 352 are described below. At the moment these defaults are not designed to be biologically accurate,
48
49 353 but rather just to provide an example of distributions. However, there are plans to improve the
50
51 354 realism and usability of the default options in future versions, by offering the user a choice between
52
53 355 common options, such as a spherical distribution for the leaf orientation.

54 356 **Leaf area density distribution** By default the available leaf area is distributed equally to all
55
56 357 the last cylinders in the branches of the QSM. All other cylinders remain leafless.

Leaf orientation distribution The default LOD is such that most of the leaf area faces upwards, but there is some random variation. The LOD computes an initial leaf normal estimate as a cross product of the petiole direction and a side directions on a horizontal plane. If the initial direction differs less than 20° from a reference direction (straight up in this case), then the final normal direction is the reference direction. Otherwise, the final normal is the initial direction rotated towards the reference direction by 20° .

Leaf size distribution The default LSD samples a leaf length value from a uniform distribution with given limits. That value is then scaled with a value based on the relative height of the parent block to ensure that leaves are a little bit larger at the top of the tree.

3 Results

3.1 Leaf geometry complexity test

The `LeafModelTriangle` class enables the use of leaf basis geometries with an arbitrary number of triangles. However, the detection of intersections between leaves requires checking all those triangles which has an enormous effect on computational time. To study the effect of the number of triangles in the basis geometry, a single cylindrical block (length 1 m, radius 0.25 m) was fitted with an increasing total area of leaves. The area varied from 0.25 to 5 m² for the four basis geometries in Fig. 6. The process was repeated 10 times for each leaf area–basis geometry pair. The average computational time results are shown in Fig. 7.

When using a single triangle, generating non-overlapping leaves was very fast even with the maximum leaf area, 5 m², taking only 11 s on average. With the two-triangle quadrangle, the times increase 1.8-fold to 4.3-fold in comparison to the single triangle when moving from the lowest to the highest leaf area. For the polygon with 8 triangles, the required time was 8.1-fold already at 1 m² and 16-fold at the maximum. The respective multipliers for the 20-triangle polygon were 35.9 and a 79.7, which translate to 31 and 891 seconds, respectively.

3.2 Leaf area density distribution definitions

To demonstrate the leaf insertion algorithm, we defined the two following parametrized leaf area density distributions. While we tested other distributions and parametrizations, these two were chosen because of the low parameter count and overall simplicity.

LADD 1 initialized the last 5 % of each branch to have equal portion of leaves, then scaling these proportions with a factor dependent on the relative height of the respective cylinder. The

factor had a value of the parameter y_0 at ground level and 1 at the top of the tree. Values in between were interpolated linearly.

LADD 2 had an additional parameter to define a cut-off point along a branch. The branch did not have any leaves before this point, which was dependent on the branch order. For the stem the cut-off was at 95 %. For branch orders 4 and above, the cut-off was at y_4 , and for lower branch orders the cut-off was interpolated linearly. For cylinders after the cut-off point, the probability of leaves was interpolated linearly between zero at the cut-off and one at the tip of the branch. Furthermore, the probabilities were scaled with a factor depending of relative cylinder height as with LADD 1. The scaling factor y_4 is visualized in Fig. 8 for parameter value 0.4.

To find optimal values for the parameters, we performed a simple grid search by varying the values of y_0 and y_4 in the closed intervals $(0, 1)$ and $(0, 0.9)$, respectively. For LADD 1 which only depends on the y_0 parameter, the results are shown in Fig. 9, for LADD 2 the optimal parameter values are listed in Table 3. Optimization was done on the cumulative area difference that was computed as the sum of unsigned leaf area differences in the vertical layers of the trees. The error was normalized with the measured total leaf area of the tree. The total error was computed as a sum over all the trees.

For LADD 1 the total optimal value was $y_0 = 0.2$, which was close to those of the small and large oak trees. However, the optimal value of the medium oak tree was different at 0.7. For LADD 2 the total optimum values were $y_0 = 0.2$ and $y_4 = 0.5$, but there were differences in the optimal parameter values between the individual trees.

Fig. 10 visualizes the LADD 2 distribution with the optimal parameter values on the small and medium oak trees. Gray parts have no leaves, green parts have some, and red parts have a lot of leaves. Furthermore, Fig. 11 shows similar LADD heat-maps and corresponding generated leaves. Note that in Fig. 11 LADD 1 is the same as LADD 2 with parameter value $y_4 = 0.95$. Going from top to bottom the regions of high probability of leaves spread from the very tip towards the base of the branch. In the top two rows, the leaves are very concentrated to the tips, whereas in the latter two the leaves are more evenly spread along the high order branches.

3.3 Leaf insertion test for oak trees

Each of the three oak trees were inserted with their measured leaf area (highlighted in Table 1). The two LADDs described above with the optimal parameters were used, and all tree-LADD pairs were repeated ten times. As we lacked reference data for the leaf orientation and leaf size distributions, defaults from the MATLAB implementation were used. To match the measured leaf sizes for each tree, the limits for the default uniform leaf length distribution were derived from the

average leaf area measurements. The mean leaf length l_i for tree i was computed as follows:

$$l_i = \frac{\sqrt{A_i}}{r/2}, \quad (1)$$

where A_i is the average leaf area for tree i , $r \approx 0.6$ is the ratio between the width and length of the leaf basis geometry, which in this case was the quadrangle from Fig. 6 to keep the triangle count low. The leaf length limits were computed for each tree as a $l \pm 1$ cm.

The computations were done on a quad-core computer (Intel Core i7-6700K 4GHz, 32 Gb RAM). The computational mean times and standard deviations over the ten repeats are listed in Table 4. The average computational time per QSM block was between 20 and 40 ms for all the trees. Most of the computational time (95.3 %) was spent on detecting intersections, which further supports using the simplest possible leaf basis geometry. The table also lists the average number of required block and leaf neighbour computations, the average number of performed transformations to avoid intersections, and the discarded leaf candidate percentage. The small oak tree had twice the leaf area per branch in comparison to the other two trees, which explains why there were twice as many neighbouring leaf computations and discarded leaves. The results suggest that it would be sufficient to sample 5–10 % more leaves than the target leaf area to account for discarded leaves. The results show that the vast majority of leaf candidates are accepted without any transformation as the average number of tried configurations was between 1.0 and 1.5 for all the trees.

Fig. 12 shows a top view of all the oak trees with leaves generated with both LADDs, and Fig. 13 shows a side view of the LADD 1 generated leaf covers for the medium and large oaks. The differences between the leaf covers generated with LADD 1 and LADD 2 are subtle, but noticeable. As the higher order branches have a lower cut-off point along the relative position on the branch, leaf cover is more even, making the gap fraction smaller on LADD 2 covers.

To compare the generated leaf distributions to the measured data, the leaves were placed in the same vertical bins listed in Sect. 2.1 according to their centre. The signed difference between generated and measured leaf count and area are listed in Table 5. Negative values mean that the tree or layer should have had more leaves or leaf area, positive values are the opposite. Both LADDs were able to match the measured leaf area on tree-level because that was the stopping condition. The tree-level leaf counts are only between 500 and 3500 below the target values. Relative to the total leaf count the differences were 7.5 %, 0.9 % and 2.0 % for the small, medium and large oaks, respectively.

The layer-level differences were much higher, which suggests that the vertical distribution generated by the proposed LADDs did not match the measurements. With LADD 2 the top layer of the large oak was missing over 90 m² of leaf area while the layer below that had an excess of

1
2 455 about 60 m². Results for the small oak were similar, which suggests lowering the y_0 parameter.
3
4 456 However, the opposite was true for the medium oak, which had about 6 m² of extra leaf area in the
5 457 upper layer.
6
7
8

9 458 **4 Discussion**

11 459 The above results presented two relatively simple LADD functions that used branch order, relative
12 460 height and relative position along a branch to determine the portion of leaf area to be assigned to
13 461 a block. However, the implementation allows for the user to write more complex LADD functions
14 462 that make use of additional information, such as, absolute height (whether the block is above the
15 463 surrounding canopies) and absolute orientation (north or south side of the stem). Due to limited
16 464 reference data only the LADD was optimized. However, if detailed leaf angle or leaf size measure-
17 465 ments are available, it is possible to optimize the respective distribution in a similar manner.
18
19

20 466 The LADD parameter optimization results and the conflicting layer difference results show that
21 467 the presented LADDs are not able to capture the differences in the leaf area distributions of the
22 468 three oaks trees. Further studies should be made to assess whether the underlying leaf distribu-
23 469 tions differ between these three trees, or whether it is simply a matter of choosing a better LADD.
24 470 It should also be noted that the manual leaf measurements were limited with only 8 data points in
25 471 total for the three trees, and as such, more detailed and comprehensive measurements would be
26 472 beneficial. Some of the leaf area difference can also be explained by uncertainties in estimating
27 473 leaf area and count for the vertical layers, and by missing branches in the upper canopy in the
28 474 QSMs.
29

30 475 The parameters of the two LADDs were optimized by using a grid search where exact leaf
31 476 geometry was generated at each grid position. This made the optimization computationally inten-
32 477 sive as 95 % of the computational time was spent on intersection prevention, which forced a low
33 478 parameter count. However, in retrospect it was unnecessary to generate leaf geometry, because
34 479 as the results showed the discard rate was very low, which means that the LADD of the output
35 480 was very close to the input. Thus, optimization according to, *e.g.*, vertical layers can be simplified
36 481 to only include distributing the available leaf area onto the structure model and exclude both leaf
37 482 size and orientation sampling and especially the computation of exact geometry.
38

39 483 Future research should also include testing the importance of the intersection prevention for
40 484 various applications, *i.e.*, whether possibly intersecting and non-intersecting leaves differ signifi-
41 485 cantly in terms of required resources and produced level of detail. This way we would know
42 486 whether it is sensible to perform the intersection prevention step, *e.g.*, for simulations studying
43 487 light use efficiency.
44

45 488 In this paper, the proposed method was only used to generate leaf covers according to user-
46
47
48
49
50
51
52
53
54
55
56
57
58
59
60

1
2 489 given distributions. However, also interesting would be to see if this algorithm could be used
3
4 490 to invert or approximate the real-leaf distributions of a given tree, with simple non-destructive
5
6 491 and non-direct measurements. For example, it would be possible to test whether gap-fraction
7
8 492 measurements and suitable parametrizations of the leaf distributions can be used to optimize the
9
10 493 distribution parameters, to derive a mathematical or even a biological explanation for the real leaf
11
12 494 distribution. With the method, it is possible make such simulations and study this inverse problem.
13
14 495 It should be noted, that such inversion does not reconstruct exact leaf geometry but rather gives an
15
16 496 approximation of their distributions. Such an approach could produce new understanding of what
17
18 497 affects the distribution of leaves for a specific tree. Furthermore, it would allow the generation of
19
20 498 leaf covers that follow the reconstructed distribution for the same tree or some other tree.

21
22 499 Currently the algorithm views each leaf independent from the others (apart from intersection
23
24 500 prevention), which is one of the reasons for calling the algorithm naïve. However, in most tree
25
26 501 species leaves follow a certain phyllotaxy or the leaves are clumped together, *e.g.*, their petioles
27
28 502 originate near one another, or even from the very same spot [23]. We are planning to implement
29
30 503 simple phyllotaxy controls in future versions of the FaNNI implementation. The level of clumping
31
32 504 could be defined as a separate distribution, that would be used to sample the size of a clump and
33
34 505 variation in petiole and leaf parameters for the leaves within the clump.

35
36 506 In nature leaves are often connected to branches that are small in diameter. Because of the
37
38 507 limitations of the TLS technology, such branches are often poorly sampled in the resulting point
39
40 508 clouds. Therefore, they can be excluded from the reconstructed QSM also, which means that
41
42 509 when leaves are inserted, they are connected to branches that are too large. To counter this
43
44 510 shortcoming, it is possible to perform a pre-processing step that inserts small branches to the
45
46 511 structure model, which will be given a high probability of leaves when defining the LADD function.

47
48 512 Although the implementation enables the use of leaf basis geometries consisting of any number
49
50 513 of triangles, the results show that additional complexity multiplies the expected computational
51
52 514 time by large factors. However, if detailed leaf geometry is required for later computations, it
53
54 515 is possible to use a simplified stand-in basis geometry that encapsulates the complex shape to
55
56 516 prevent overlapping during generation, and replace the geometry afterwards. Such a procedure
57
58 517 could even be build-in to an extension of the `LeafModel` class.

51 518 **5 Conclusion**

52
53
54 519 We have presented an algorithm to generate non-intersecting leaves to a QSM, that follow user-
55
56 520 defined position, size and orientation distributions. A MATLAB implementation of the algorithm was
57
58 521 also presented. Currently, the implementation allows the use of any leaf shape consisting of an
59
60 522 arbitrary number of triangles.

1
2 523 In order to present leaf property distributions in a compact yet versatile format, we propose a
3
4 524 scheme where a QSM is divided into blocks that determine, and can be used to contain, property
5
6 525 information for leaves that are to be connected to it. This means that we can assign the available
7
8 526 leaf area, leaf size and orientation parameters to the blocks of a QSM even without generating
9
10 527 leaves. Then we can do one of the following:

- 11 528 • Visualize the property distributions by colouring the blocks according to their respective prop-
12 529 erty values as seen in the case of leaf area density distributions, *e.g.*, in Figs. 10 and 11.
- 13
14 530 • Sample the user-defined distribution with the parameter values and generate exact leaf ge-
15 531 ometry as was done in Sect. 3.
- 16
17 532 • View the leaves as a probability distribution around the QSM blocks, and rather than com-
18 533 puting exact leaf geometry do computations by determining a probability of a hit and the
19 534 incidence angle when a beam enters the vicinity of a block.

20
21
22 535 Although any triangle-based geometry is possible for the leaves, a simple test of adding an
23 536 increasing area of leaves to a single cylindrical block showed that complex leaf shapes can dras-
24 537 tically increase the computational time, at least with the current implementation. Thus, the leaf
25 538 basis geometry should be kept as simple as possible, or optimization is required for intersection
26 539 detection.

27
28
29 540 To demonstrate leaf generation, we presented two different LADDs and applied them to three
30 541 oak trees trying to match field measured leaf count and areas. The measurements were done
31 542 with 2 to 4 vertical bins per tree, and the average leaf area was also recorded for each tree.
32 543 Simple uniform leaf size distribution (with some scaling based on height) and planophile orientation
33 544 distribution were used, while the main focus was on optimizing the LADDs. The two suggested
34 545 LADDs were able to match leaf area and count per tree, but the vertical distribution of leaves had
35 546 major errors despite the optimization. Further research is required to understand the cause of the
36 547 leaf area differences.

37 548 A further goal is to use the leaf-augmented QSM (L-QSM) to incorporate a number of biological
38 549 principles such as the availability of resources (mass and energy exchanges between vegetation
39 550 and atmosphere, and phyllotaxy) to construct as self-consistent tree models as possible. One can
40 551 include stochastic variations in the same sense as in the creation of 4D QSMs [24], extending that
41 552 scheme to fully functional trees. This approach would enable a large number of applications to
42 553 verify and refine assumed biological postulates of theoretical models, and then use the resulting
43 554 full-scale 3D and 4D models for predictions and the modelling of ecological systems at various
44 555 size and complexity scales, including large-scale statistical (allometric) estimates.

Data Accessibility

The MATLAB implementation of the FaNNI-algorithm is available on GitHub (<https://github.com/InverseTampere/qsm-fanni-matlab>). The three oak tree QSMs are available from Eric Casella (Eric.Casella@forestry.gsi.gov.uk) upon request, until they are made public, pending the release of an unrelated study.

Authors' contributions

Markku Åkerblom developed the FaNNI algorithm, wrote the implementation, carried-out the computations, and drafted the manuscript. Eric Casella acquired the TLS measurements, computed the QSMs and led the destructive leaf sampling experiment. Mathias Disney, Mark Danson, Rachel Gaulton and Lucy Schofield participated in that experiment. Pasi Raunonen, Mikko Kaasalainen, Eric Casella, Mathias Disney, Mark Danson, Rachel Gaulton and Lucy Schofield helped draft the manuscript. All authors gave final approval for publication.

Acknowledgements

The following additional people participated in the oak tree leaf measurements: Ian Craig, Steve Coventry, Marc Sayce and David Payne from the Forest Research UK; Andrew Burt, Ross Hawton, Jingjing Yan and Meng Yu from the University College London; Ewan Pinnington from the University of Reading; and Amy Danson and Jennifer Danson.

This study was funded by the Academy of Finland research project *Centre of Excellence in inverse problems* [284715], and by the Forestry Commission GB.

Competing interests

The authors have no competing interests.

References

- [1] Casella E, Sinoquet H. Botanical determinants of foliage clumping and light interception in two-year-old coppice poplar canopies: assessment from 3-D plant mock-ups. *Annals of Forest Science*. 2007;64(4):395–404. Available from: <https://doi.org/10.1051/forest:2007016>.

- 1
2 582 [2] Newnham GJ, Armston JD, Calders K, Disney MI, Lovell JL, Schaaf CB, et al. Terrestrial Laser
3 Scanning for Plot-Scale Forest Measurement. *Current Forestry Reports*. 2015;1(4):239–251.
4 583 Available from: <http://dx.doi.org/10.1007/s40725-015-0025-5>.
5 584
- 6
7
8 585 [3] Woodgate W, Disney M, Armston JD, Jones SD, Suarez L, Hill MJ, et al. An improved
9 theoretical model of canopy gap probability for Leaf Area Index estimation in woody
10 ecosystems. *Forest Ecology and Management*. 2015;358:303 – 320. Available from:
11 586 <https://doi.org/10.1016/j.foreco.2015.09.030>.
12 587
13 588
- 14
15 589 [4] Ross J. The radiation regime and architecture of plant stands. *Tasks*
16 for Vegetation Science. Springer Netherlands; 1981. Available from:
17 590 <http://doi.org/10.1007/978-94-009-8647-3>.
18 591
- 19
20 592 [5] Raumonon P, Kaasalainen M, Åkerblom M, Kaasalainen S, Kaartinen H, Vastaranta M, et al.
21 Fast Automatic Precision Tree Models from Terrestrial Laser Scanner Data. *Remote Sensing*.
22 593 2013;5(2):491–520. Available from: <http://dx.doi.org/10.3390/rs5020491>.
23 594
- 24
25
26 595 [6] Hackenberg J, Spiecker H, Calders K, Disney M, Raumonon P. SimpleTree—An Efficient
27 Open Source Tool to Build Tree Models from TLS Clouds. *Forests*. 2015;6(11):4245–4294.
28 596 Available from: <http://dx.doi.org/10.3390/f6114245>.
29 597
- 30
31 598 [7] Grau E, Durrieu S, Fournier R, Gastellu-Etchegorry JP, Yin T. Estimation of 3D vegeta-
32 tion density with Terrestrial Laser Scanning data using voxels. A sensitivity analysis of influ-
33 599 encing parameters. *Remote Sensing of Environment*. 2017;191:373 – 388. Available from:
34 600 <http://dx.doi.org/10.1016/j.rse.2017.01.032>.
35 601
- 36
37
38 602 [8] Disney M, Boni I, Vicari M, Burt A, Calders K, Lewis S, et al. Weighing trees with lasers:
39 603 advances, challenges and opportunities. *Interface Focus*. 2017;This issue.
- 40
41
42 604 [9] Béland M, Baldocchi DD, Widlowski JL, Fournier RA, Verstraete MM. On seeing the wood
43 from the leaves and the role of voxel size in determining leaf area distribution of forests with
44 605 terrestrial LiDAR . *Agricultural and Forest Meteorology*. 2014;184:82 – 97. Available from:
45 606 <http://dx.doi.org/10.1016/j.agrformet.2013.09.005>.
46 607
47 607
48
49
50 608 [10] Ma L, Zheng G, Eitel JUH, Moskal LM, He W, Huang H. Improved Salient Feature-
51 Based Approach for Automatically Separating Photosynthetic and Nonphotosynthetic Com-
52 609 ponents Within Terrestrial Lidar Point Cloud Data of Forest Canopies. *IEEE Trans-*
53 610 *actions on Geoscience and Remote Sensing*. 2016;54(2):679–696. Available from:
54 611 <http://dx.doi.org/10.1109/TGRS.2015.2459716>.
55 612
56
57
58
59
60

- 1
2 613 [11] Casella E, Sinoquet H. A method for describing the canopy architecture of coppice poplar
3 with allometric relationships. *Tree Physiology*. 2003;23(17):1153–1170. Available from:
4 614 <http://doi.org/10.1093/treephys/23.17.1153>.
5 615
6
7 616 [12] Béland M, Widlowski JL, Fournier RA, Côté JF, Verstraete MM. Estimating leaf
8 area distribution in savanna trees from terrestrial LiDAR measurements. *Agric-
9 617 cultural and Forest Meteorology*. 2011;151(9):1252 – 1266. Available from:
10 618 <http://dx.doi.org/10.1016/j.agrformet.2011.05.004>.
11 619
12
13 620 [13] Zheng G, Moskal LM. Leaf Orientation Retrieval From Terrestrial Laser Scanning (TLS) Data.
14 *IEEE Transactions on Geoscience and Remote Sensing*. 2012;50(10):3970–3979. Available
15 621 from: <http://dx.doi.org/10.1109/TGRS.2012.2188533>.
16 622
17
18 623 [14] Bailey BN, Mahaffee WF. Rapid measurement of the three-dimensional distribution
19 of leaf orientation and the leaf angle probability density function using terrestrial Li-
20 624 DAR scanning. *Remote Sensing of Environment*. 2017;194:63 – 76. Available from:
21 625 <http://dx.doi.org/10.1016/j.rse.2017.03.011>.
22 626
23
24 627 [15] Hétroy-Wheeler F, Casella E, Boltcheva D. Segmentation of tree seedling point clouds into el-
25 628 elementary units. *International Journal of Remote Sensing*. 2016;37(13):2881–2907. Available
26 629 from: <http://dx.doi.org/10.1080/01431161.2016.1190988>.
27 630
28
29 631 [16] Åkerblom M, Raunonen P, Kaasalainen M, Casella E. Analysis of Geometric Primitives
30 632 in Quantitative Structure Models of Tree Stems. *Remote Sensing*. 2015;7(4):4581–4603.
31 Available from: <http://dx.doi.org/10.3390/rs70404581>.
32 633
33
34 634 [17] Clawges R, Vierling L, Calhoun M, Toomey M. Use of a groundbased scanning
35 635 LiDAR for estimation of biophysical properties of western larch (*Larix occidentalis*).
36 636 *International Journal of Remote Sensing*. 2007;28(19):4331–4344. Available from:
37 <http://dx.doi.org/10.1080/01431160701243460>.
38
39
40 637 [18] Calders K, Newnham G, Burt A, Murphy S, Raunonen P, Herold M, et al. Nondestructive
41 638 estimates of above-ground biomass using terrestrial laser scanning. *Methods in Ecology and
42 639 Evolution*. 2015; Available from: <http://dx.doi.org/10.1111/2041-210X.12301>.
43
44
45 640 [19] Perttunen J, Sievänen R, Nikinmaa E. LIGNUM: a model combining the structure and
46 641 the functioning of trees. *Ecological Modelling*. 1998;108(1–3):189 – 198. Available from:
47 642 [https://doi.org/10.1016/S0304-3800\(98\)00028-3](https://doi.org/10.1016/S0304-3800(98)00028-3).
48
49
50 643 [20] Disney M, Lewis P, Saich P. 3D modelling of forest canopy structure for remote sens-
51 644 ing simulations in the optical and microwave domains. *Remote Sensing of Environment*.
52 645 2006;100(1):114 – 132. Available from: <https://doi.org/10.1016/j.rse.2005.10.003>.
53
54
55
56
57
58
59
60

- 1
2 646 [21] Cannell MGR, Bowler KC. Phyllotactic arrangements of needles on elongating conifer shoots:
3 a computer simulation. Canadian Journal of Forest Research. 1978;8(1):138–141. Available
4 647 from: <http://dx.doi.org/10.1139/x78-022>.
5 648
- 6
7 649 [22] Åkerblom M. QSM-FaNNI Matlab implementation source code; 2017.
8
9 650 <https://doi.org/10.5281/zenodo.800496>.
- 10
11 651 [23] Niklas KJ. The Role of Phyllotatic Pattern as a” Developmental Constraint” On the
12 Interception of Light by Leaf Surfaces. Evolution. 1988;42(1):1–16. Available from:
13 652 <https://doi.org/10.2307/2409111>.
14 653
- 15
16 654 [24] Potapov I, Järvenpää M, Åkerblom M, Raunonen P, Kaasalainen M. Data-based stochastic
17 modeling of tree growth and structure formation. Silva Fennica. 2016;50(1). Available from:
18 655 <http://dx.doi.org/10.14214/sf.1413>.
19 656
20
21
22
23
24
25
26
27
28
29
30
31
32
33
34
35
36
37
38
39
40
41
42
43
44
45
46
47
48
49
50
51
52
53
54
55
56
57
58
59
60

Table 1: Leaf area and count measurements.

Tree / Layer	Leaf area [m²]	Leaf count
Small oak	153	47644
0.0 – 11.5 m	18	5432
11.5 – 19.6 m	135	42212
Medium oak	215	52416
0.0 – 9.0 m	46	12753
9.0 – 19.9 m	169	39663
Large oak	339	114224
0.0 – 8.0 m	61	16056
8.0 – 13.0 m	23	9399
13.0 – 18.4 m	49	19597
18.4 – 22.4 m	206	69172

Table 2: Oak tree properties computed from reconstructed QSMs.

Property	Oak tree		
	Small	Medium	Large
Branch count	1334	3579	6161
Cylinder count	8429	23539	35428
DBH [mm]	298	432	848
Height [m]	19.1	19.6	21.8
Order max.	9	8	9
Total length [m]	592	1552	2516
Volume [l]	707	1169	2098

Table 3: Optimal parameter values for LADD 2 distribution. Parameter y_0 controls vertical distribution and parameter y_4 distribution along branch length.

Tree	y_0	y_4
Small oak	0.1	0.7
Medium oak	0.6	0.5
Large oak	0.2	0.9
Total	0.2	0.5

1
2
3
4
5
6
7
8
9
10
11
12
13
14
15
16
17
18
19
20
21
22
23
24
25
26
27
28
29
30
31
32
33
34
35
36
37
38
39
40
41
42
43
44
45
46
47
48
49
50
51
52
53
54
55
56
57
58
59
60

Table 4: Oak tree average leaf generation results. The properties are computational mean time, time standard deviation, average block and leaf neighbour counts and average number of transformation configurations tried before accepting or discarding a leaf.

Tree / LADD	Time	Time std	Block neigh.	Leaf neigh.	Transforms	Discard
LADD 1						
Small oak	6 min 12 s	7 s	13.1	32.8	1.4	7.3 %
Medium oak	7 min 55 s	9 s	15.7	16.3	1.0	3.4 %
Large oak	17 min 48 s	30 s	11.8	16.2	0.9	3.5 %
LADD 2						
Small oak	6 min 32 s	4 s	13.6	33.9	1.4	7.8 %
Medium oak	8 min 07 s	5 s	16.1	16.2	1.0	3.6 %
Large oak	18 min 19 s	8 s	12.4	16.5	1.0	3.6 %

Table 5: Difference between oak leaf count and leaf area in total and in vertical layers.

Tree / Layer	LADD 1		LADD 2	
	Δ Count	Δ Area [m ²]	Δ Count	Δ Area [m ²]
Small oak	-3561	+0.0	-3581	+0.0
0.0 – 11.5 m	+1707	+5.7	+1002	+3.3
11.5 – 19.6 m	-5268	-5.7	-4583	-3.3
Medium oak	-473	+0.0	-432	+0.0
0.0 – 9.0 m	-3339	-8.1	-2811	-6.0
9.0 – 19.9 m	+2866	+8.1	+2379	+6.0
Large oak	-2275	-0.1	-2157	+0.0
0.0 – 8.0 m	+9507	+12.9	+10748	+16.6
8.0 – 13.0 m	+2758	+13.1	+3254	+14.5
13.0 – 18.4 m	+15634	+58.7	+15883	+59.4
18.4 – 22.4 m	-30174	-84.8	-32040	-90.5

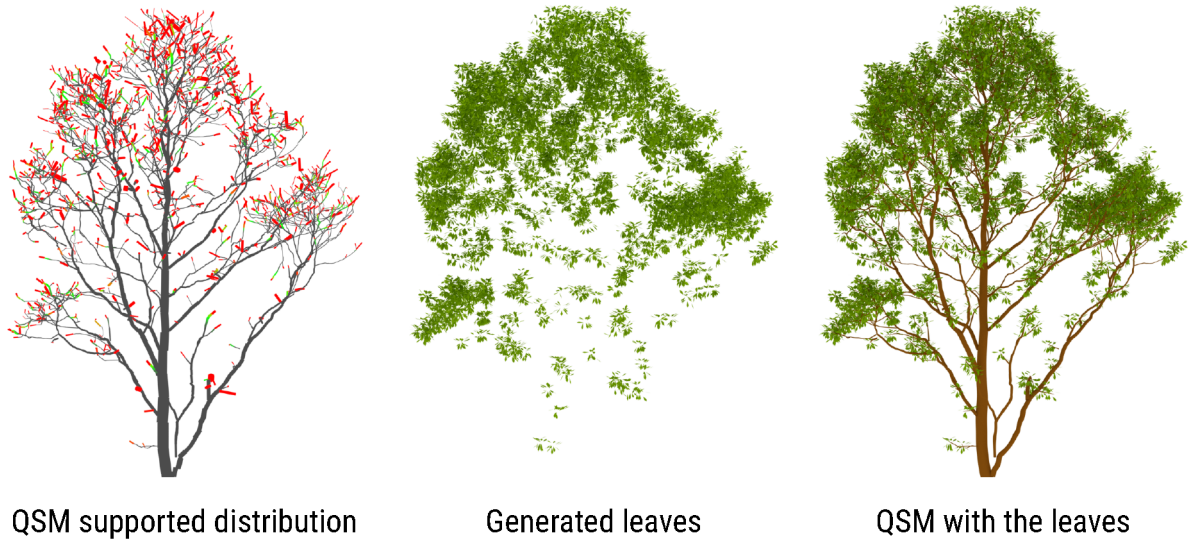


Figure 1: A QSM supports a leaf area distribution (grey: no leaves, green: some leaves, red: a lot of leaves), which can be sampled to generated non-intersecting leaves, and inserted to the structure model.

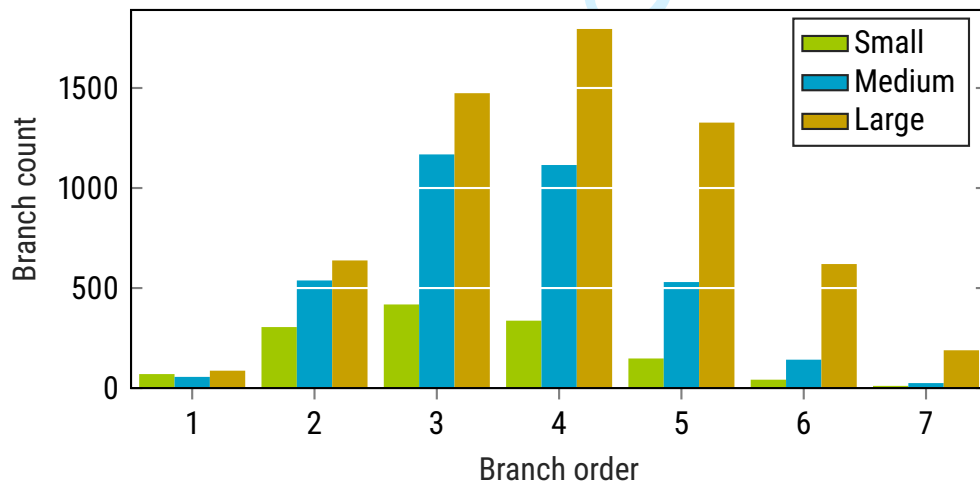
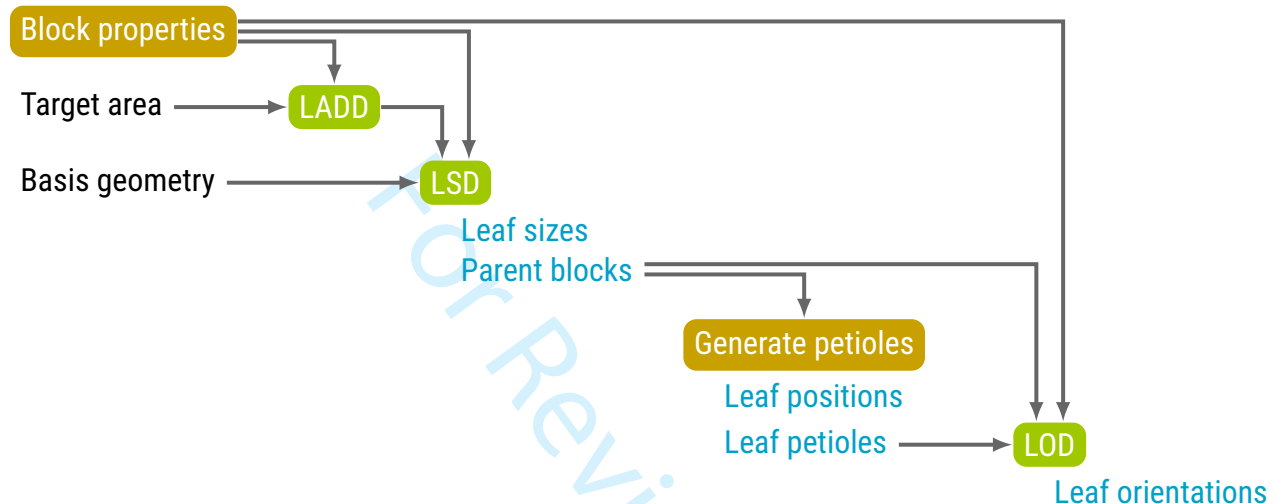


Figure 2: Branch order–count distribution. The stem and branch orders 8 and 9 have been excluded due to their negligible portions.

1
2
3
4
5
6
7
8
9
10
11
12
13
14
15
16
17
18
19
20
21
22
23
24
25
26
27
28
29
30
31
32
33
34
35
36
37
38
39
40
41
42
43
44
45
46
47
48
49
50
51
52
53
54
55
56
57
58
59
60

I. CANDIDATE GENERATION



II. ACCEPTING CANDIDATES

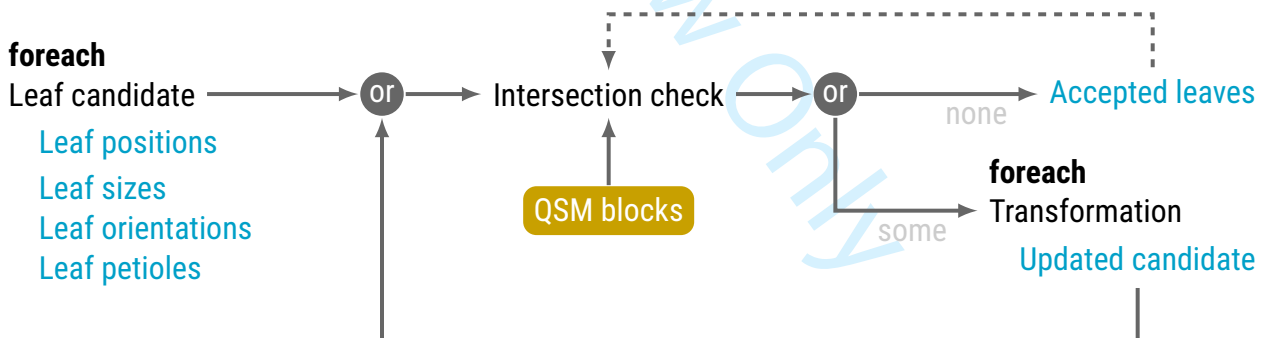


Figure 3: Process overview of the leaf generation process. Leaf distributions are drawn in green, and functions and properties related to the QSM in orange. The main outputs are written in blue. The two stages are presented on top of one-another.

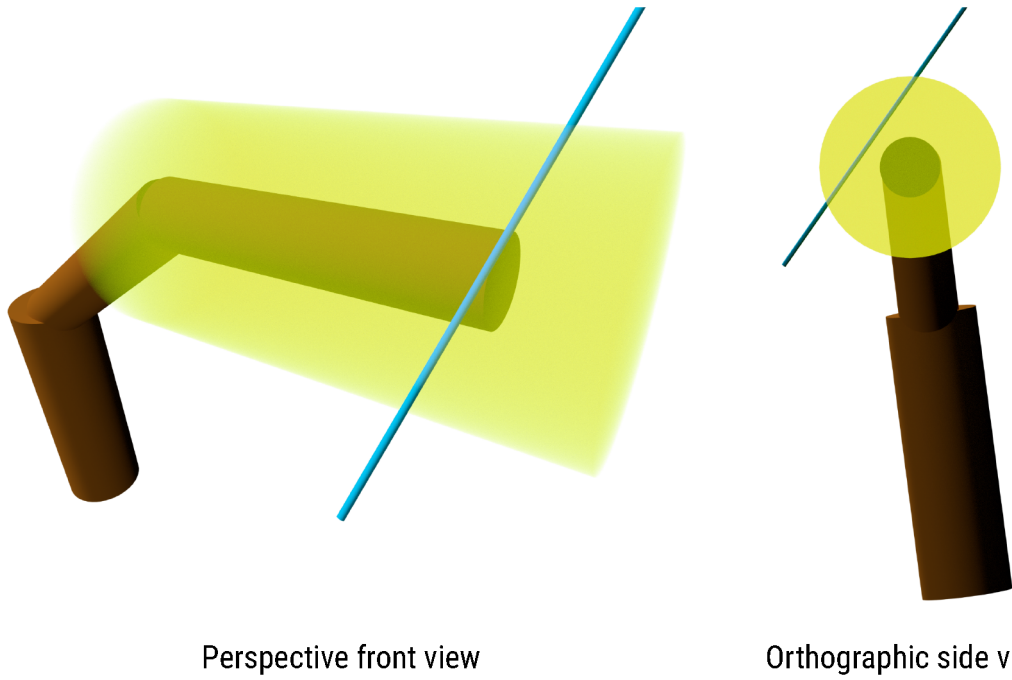


Figure 4: Two views of an example ray (blue) travelling the leaf density cylinder (yellow) that is supported by one of the branch cylinders (brown).



Figure 5: An example of a needle bud 3D model without a strict phyllotaxy.

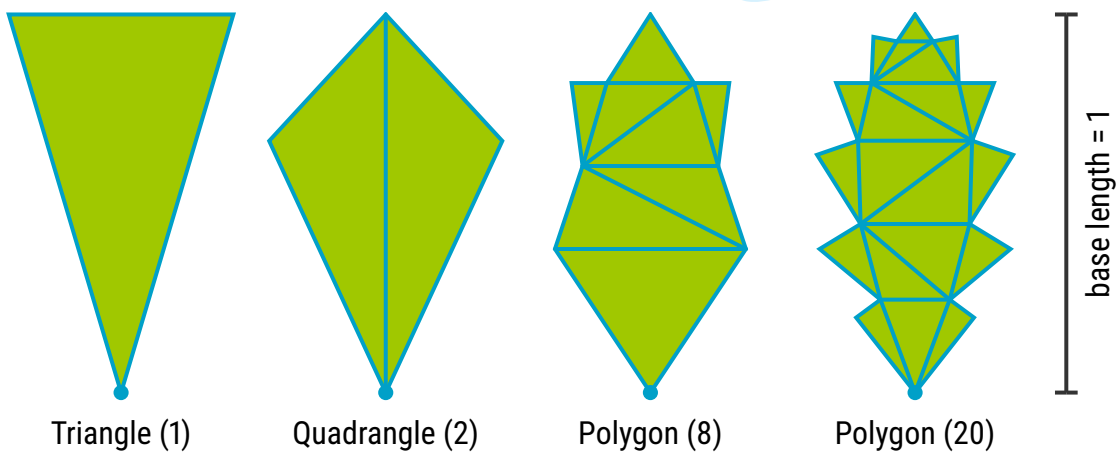


Figure 6: Triangular basis leaf geometries. The number of triangles is given in parenthesis. The origin of the leaf is marked with a circle, and the length of a basis geometry always equals one.

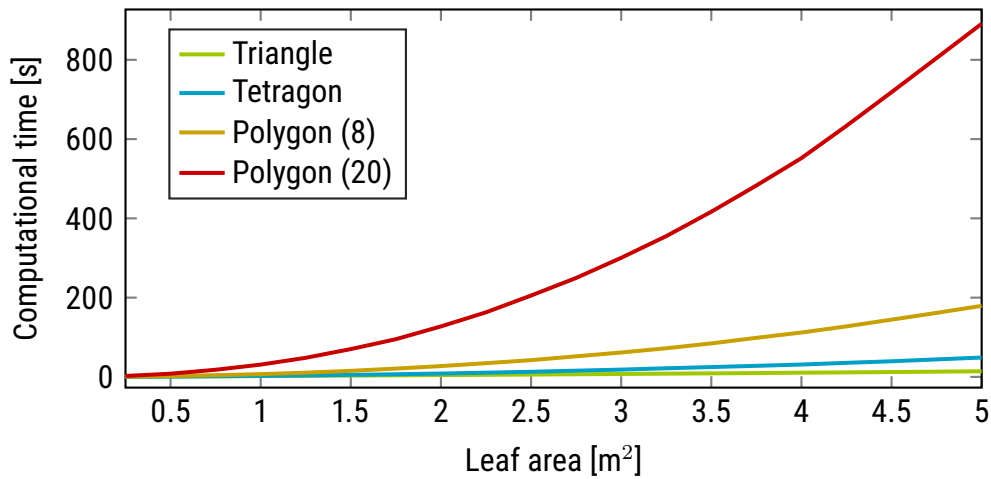


Figure 7: Computational time as a function of total generated leaf area for a single test cylindrical block. The values are averages over the ten repeats.

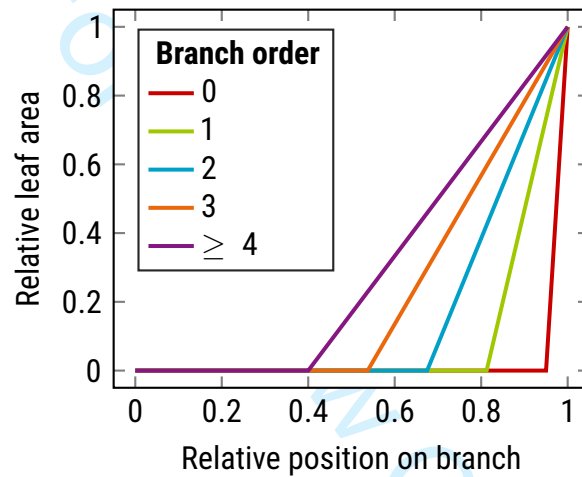


Figure 8: Piecewise linear polynomials defining the branch order-dependent LADD 2 scaling factor $y_4 = 0.4$.

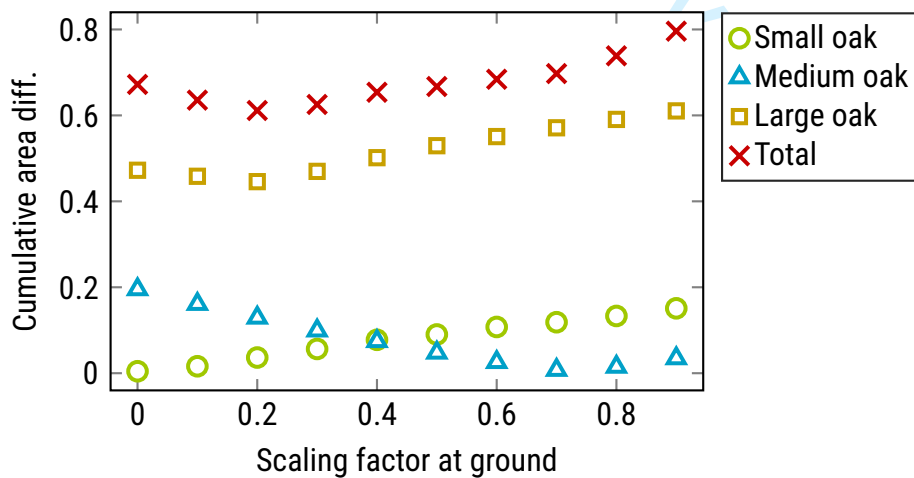
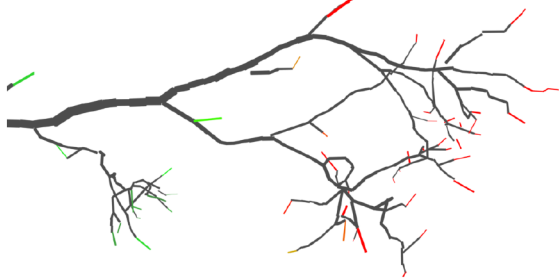


Figure 9: Cumulative area difference curves for LADD 1 distribution as a function of the height scaling parameter.

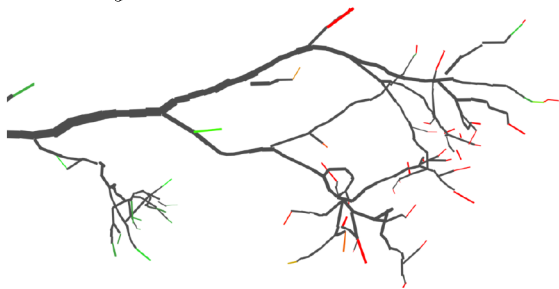


Figure 10: Example leaf area density distribution (LADD 2) for the small and medium oak trees as heat maps. As branch tips are small in size all cylinder radii have been scaled up to 4 times larger according their LADD value for a better visualization.

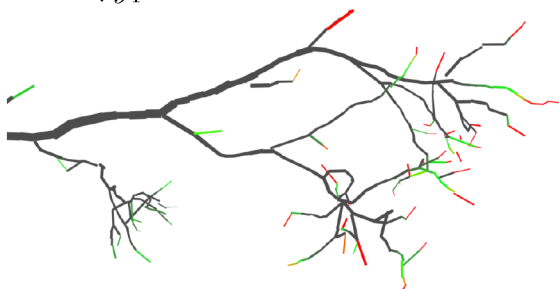
LADD 1 / LADD 2, $y_4 = 0.95$



LADD 2, $y_4 = 0.9$



LADD 2, $y_4 = 0.5$



LADD 2, $y_4 = 0.1$

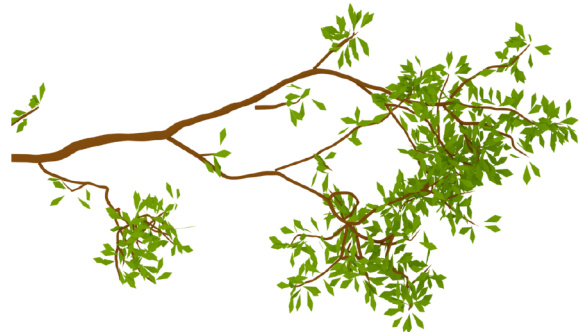
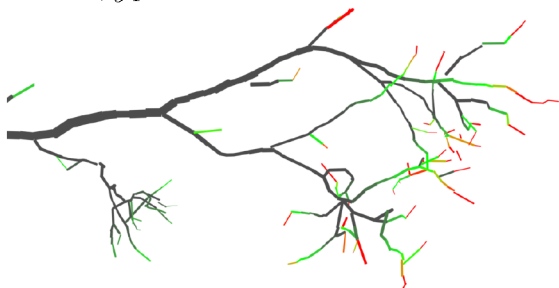


Figure 11: LADD examples on a single branch from the small oak tree. The distributions control how leaf area is distributed on the supporting branching structure. The parameter y_4 controls the cut-off point along the branch length, starting from the branch base, before which there can be no leaves. Left: distribution as a heat map, Right: sampled leaves based on the corresponding heat map.

1
2
3
4
5
6
7
8
9
10
11
12
13
14
15
16
17
18
19
20
21
22
23
24
25
26
27
28
29
30
31
32
33
34
35
36
37
38
39
40
41
42
43
44
45
46
47
48
49
50
51
52
53
54
55
56
57
58
59
60

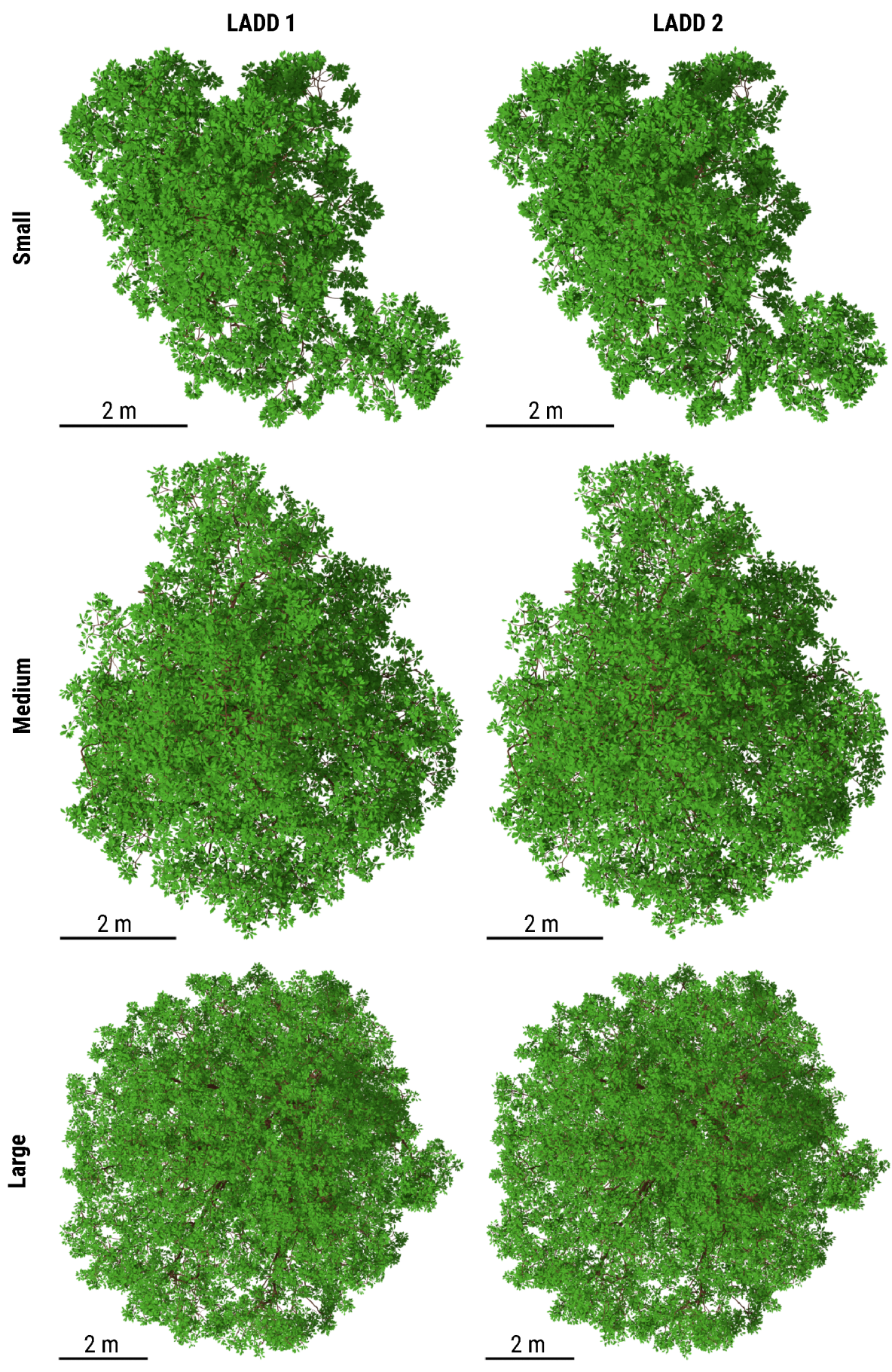


Figure 12: Top view of the three oaks with leaves generated with the two LADDs.

1
2
3
4
5
6
7
8
9
10
11
12
13
14
15
16
17
18
19
20
21
22
23
24
25
26
27
28
29
30
31
32
33
34
35
36
37
38
39
40
41
42
43
44
45
46
47
48
49
50
51
52
53
54
55
56
57
58
59
60



Figure 13: Side view of the medium and large oak with leaves generated with LADD 1.